PROCEEDINGS OF SCIENCE

# First operation of superconducting quantum bits as particle detectors

**Camilla Bonomo,**[a,b,*] **Mustafa Bal,**[e] **Nicola Casali,**[b] **Ivan Colantoni,**[b,f] **Francesco Crisa,**[h] **Angelo Cruciani,**[b] **Francesco De Dominicis,**[c,d] **Fernando Ferroni,**[b,c] **Dounia L. Helis,**[d] **Ambra Mariani,**[b] **Yasir R. Mehmood Khan,**[c] **Lorenzo Pagnanini,**[c,d] **Valerio Pettinacci,**[b] **Roman Pilipenko,**[e] **Stefano Pirro,**[d] **Andrei Puiu,**[d] **Alberto Ressa,**[b] **Alexander Romanenko,**[e] **Tanay Roy,**[e] **Marco Vignati,**[a,b] **David v Zanten,**[e] **Shaojiang Zhu,**[e] **Anna Grassellino**[e] **and Laura Cardani**[b]

[a] *Dipartimento di Fisica, Sapienza Università di Roma, Piazzale Aldo Moro 2, Roma, Italy*
[b] *INFN – Sezione di Roma, Piazzale Aldo Moro 2, Roma, Italy*
[c] *Gran Sasso Science Institute, L'Aquila I-67100, Italy*
[d] *INFN – Laboratori Nazionali del Gran Sasso, Assergi (L'Aquila) I-67100, Italy*
[e] *Superconducting Quantum Materials and Systems Center (SQMS), Fermi National Accelerator Laboratory, Batavia, IL 60510, USA*
[f] *Consiglio Nazionale delle Ricerche, Istituto di Nanotecnologia*
[g] *Illinois Institute of Technology*
[h] *Xanadu Quantum, Canada*

*E-mail:* camilla.bonomo@uniroma1.it

Transmon qubits are among the leading technologies for the development of future quantum computers. However these superconducting devices are sensitive to ionizing radiation, which reduces their coherence time and leads to correlated errors. This study represents the first quantitative estimation of cosmic rays and ambient radiation impact on transmon qubits. In the shielded underground facility at the Laboratori Nazionali del Gran Sasso (LNGS), errors induced by the interaction of a radioactive source were reconstructed with an efficiency of about 10%. In contrast, in the unshielded above-ground facility at the Fermi National Accelerator Laboratory (FNAL), cosmic and ambient radiation impacts were detected with an efficiency ranging from 10% to 20% by modifying the acquisition protocol. Lastly, the simultaneous readout of three transmons in coincidence was demonstrated, achieving an event reconstruction efficiency of 90% when the devices were illuminated with an LED.

*14th Young Researcher Meeting (14YRM2025)*
*30 September - 3 October 2025*
*Gran Sasso Science Institute, L'Aquila,*

*Speaker


ISSN 1824-8039. Published by SISSA Medialab. https://pos.sissa.it/

PoS(14YRM2025)001

## 1. Introduction

Quantum bits (qubits) based on superconducting technology represent the state of the art in quantum information science. Among all superconducting qubits, transmons have become the current standard, because they offer a good balance between coherence time and ease of control and fabrication. A transmon qubit can be modelled as a two-level system: a quantum state measurement yields either the ground state $|0\rangle$ or the excited state $|1\rangle$.
It has been shown that transmon qubits are sensitive to ionizing radiation, including both natural radioactivity and cosmic rays [1, 2]. Such radiation interferes with their quantum behaviour, drastically reducing their coherence time, i.e. the period during which they maintain quantum properties. This can lead to correlated errors [3], which limits quantum information processing, because such errors cannot be corrected by standard error-correction algorithms that assume spatially and temporally independent errors. However, this sensitivity could also be seen as an opportunity for particle detection, as explored in this work.

## 2. Experimental Apparatus

The core component of the experimental apparatus is the chip, shown in Figure 1a, housed in a gold-plated copper box. The $7.5 \times 7.5$ mm$^2$ chip consists of eight niobium transmons with

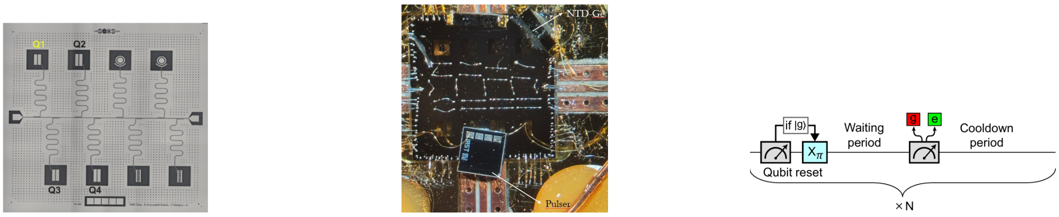


**(a)** Single-readout **(b)** Multiplexing **(c)** Fast reset

**Figure 1:** Figure 1a: The chip containing eight niobium transmon qubits analysed in the single readout datasets [4]. Figure 1b: The eight-transmon chip analysed in the multiplexed readout, equipped with an NTD-Ge thermistor and a heater. Figure 1c: Schematic representation of the fast reset detection protocol [4].

aluminum Josephson junctions on a 432 $\mu$m sapphire substrate, covered with a niobium layer serving as a ground plane [4]. Devices are gold-capped to prevent niobium oxidation and operated in a dilution cryostat at 10 mK within a Cryoperm® magnetic shield. The chip fabrication, including substrate preparation, niobium layer deposition, and Josephson junction evaporation, followed the procedure described in Ref. [5]. Each qubit is coupled to an LC-resonator, consisting of a spiraling superconducting capacitor, whose inductance is determined by its geometry.

## 3. Signal Generation and Detection Protocol

In this work, the reconstructed signal relies on a phonon-mediated approach. The particles of interest are cosmic muons and ambient photons, originating from natural radioactivity, including the decay chains of $^{232}$Th, $^{238}$U and $^{235}$U, as well as the decay of $^{40}$K, with energies ranging from a few keV up to 2.6 MeV. Both muons and photons interact with the sapphire substrate, which

constitutes the bulk part of the chip: muons primarily through ionization, the photons through photoelectric effect and Compton scattering. These interactions generate electron-hole pairs in the substrate, whose recombination produces high-energy phonons. The phonons then scatter in the substrate, losing energy and producing lower energy phonons, which reach the superconducting islands of the transmon. If their energy is close to $2\Delta$ ($\Delta$ being the superconducting gap), they can break Cooper pairs, producing quasiparticles that may tunnel through the Josephson junction. This acts as an energy loss channel, causing the immediate decay of the transmon, if it had been previously excited. Phonon propagation reduces the probability of qubit re-excitation.
This forms the basis of our detection protocol, referred to as the fast reset, illustrated in Figure 1c. The first step consists of reading the transmon state: if it is found in the ground state, it will be excited. After a delay time $t_d$ of a few microseconds, the transmon state is read again, and the entire protocol is repeated after a cool-down period of tens of microseconds. Transmon readout follows Refs. [4, 7]. Although treated as two-level systems, transmons can leak into higher energy states during the protocol. To prevent misclassification, high-leakage events were excluded. In the first runs, the live-time was heavily reduced, preserving only about 20% of the run, in order to obtain a clean sample. Later, after optimizing the readout protocol, the live-time improved up to 100%. The outcome of the measurements is a stream of zeros and ones.



## 4. Single-qubit Readout Analysis

In this section, the analysis of single-qubit readout datasets is presented. The datasets were collected in two different experimental facilities. At the Laboratori Nazionali del Gran Sasso (LNGS), the chip was fully shielded from ambient radioactivity by lead and copper bricks, the latter used to suppress lead-induced gamma rays, and from cosmic rays by the Gran Sasso rock overburden. A signal event is expected to be characterized by the detection of a large number of zeros within a short time interval, as a consequence of the phonon-mediated relaxation processes described previously. Therefore, the analysis focuses on the study of the number of zeros in the signal region for triggered events, flagged after the detection of four consecutive zeros. Each acquisition window is divided into a control and a signal region, and the event selection is based on requiring a minimum number of zeros $Z_{min}^{sig}$ in the latter, in order to suppress events dominated by spontaneous qubit relaxation. The signal region serves as dead time, to avoid triggering multiple times on the same event. The probability for spontaneous decay is given by $P_g \approx t_d/T_1$, with $T_1 \approx 80\ \mu$s the effective relaxation time, and the trigger rate of four consecutive ground detection induced by the decay is $P_g^4/T_s$ results in few events per second, with $T_s$ the sampling period [4]. Additional cuts are applied to the control region to discard noisy events. The selection procedure is thoroughly described in Refs. [4, 7]. The qubit state readout is a Bernoulli process with just two possible outcomes: $|0\rangle$ and $|1\rangle$, each occurring with a different probability. As a consequence, the distribution of zeros can be modelled with a binomial distribution. The probability of detecting $x$ false positives in $n$ repeated measurements in the signal region, each corresponding to a data point, is:

$$f(x; n, P_g) = \binom{n}{x} P_g^x (1 - P_g)^{n-x} \tag{1}$$

More precisely, to compute $Z^{sig}_{min}$, we consider the cumulative binomial distribution, computed varying $x$ in the interval $0-40$ until the rate for finding more than $x$ false positives drops below the target rate $10^{-4}$ ev/sec.

### 4.1 LNGS: Radioactive source impact

In the fully-shielded LNGS configuration, it was possible to evaluate the impact of $^{232}$Th sources with different activities, placed between the cryostat and the lead shield. Figure 2a shows

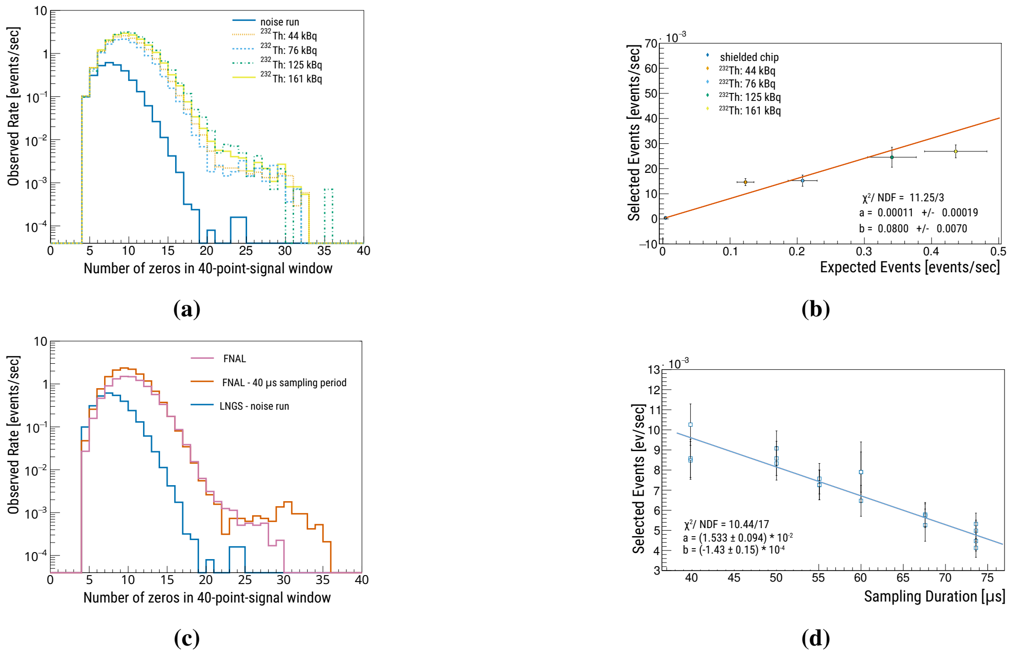


**Figure 2:** Figure 2a: distribution of the number of zeros in the signal window for triggered events. Figure 2b: Scatter plot of simulated rate of photons impinging on the substrate versus the measured rate of selected events, for different source activities. Figure 2c: comparison of the number of zeros in the signal window between LNGS and Fermilab runs. Figure 2d: rate of selected events as a function of the sampling period.

the distribution of the number of zeros in the signal window for triggered events. The left-hand side of the histogram follows a binomial distribution, corresponding to zeros arising from spontaneous decay of the qubit. On the right-hand side, an excess is observed when comparing the runs performed without radioactive sources with those acquired with the sources in place. This excess can be explained by considering that, as long as the phonons produced by a radiation-induced event continue to interact with the active part of the qubit, the excited transmon will decay immediately. As a consequence, repeated detections of the ground state are expected during phonon propagation in the substrate. In Figure 2b, the selected event rates are shown as a function of the expected ones. The ratio between the two, which can be extraxted from the slope of the fit, corresponds to efficiency. The estimated overall efficiency for reconstructed signal events is (8 ± 0.7 (stat.) ± 2.4 (syst.) )%. The systematic uncertainty is dominated by the conversion of the points in the I-Q plane (with I, Q being the components of the complex readout signal) into the stream of 0s and 1s, due to the readout noise and to the population of higher-energy states. The threshold for state determination

PoS(14YRM2025)001

is set on the I value. By repeating the same analysis with a more or less aggressive selection, the variations in the efficiency remained below 30%, assumed to be the systematic uncertainty.

### 4.2 FNAL: Cosmic muons and ambient photons impact

In this experimental configuration, the chip is unshielded, therefore it was possible to quantify the effect of cosmic muons and environmental photons on the chip. Figure 2c shows the distribution of the number of zeros for the shielded LNGS run, compared with two runs acquired in the unshielded FNAL facility. The expected event rate from simulation in the latter case is $(42 \pm 3) \cdot 10^{-3}$ events/s [4]. The solid pink line corresponds to a FNAL run acquired with the same sampling period as the shielded LNGS run (blue histogram). In this comparison, the excess of zeros in the right tail of the FNAL distribution is attributed to the impact of cosmic rays and environmental photons. Nevertheless, it was not possible to disentangle the two contributions. The expected external photon rate was $(31 \pm 2) \cdot 10^{-3}$ [ev/sec], whilst the expected muon rate was $(8.0 \pm 0.5) \cdot 10^{-3}$ [ev/sec] [4]. The red histogram corresponds to a run acquired with a shorter sampling period, where a larger number of zeros is observed. In Figure 2d, the rate of selected events is plotted as a function of the sampling period. It can be observed that the efficiency in reconstructing signal events nearly doubles from 10% to 20% when the sampling period is reduced, from 73.6 $\mu$s to 39.8 $\mu$s. The faster the sampling, the higher the probability of detecting zeros, since the sampling period lasts on the order of microseconds, while phonon propagation persists on the order of milliseconds. Nevertheless, reducing the sampling period also increases the probability of exciting higher energy levels of the system.

## 5. Multiplexing

This run was performed at the LNGS facility in an unshielded configuration. The chip was equipped with an NTD-Ge thermistor for independent energy estimation, and a pulser for thermal gain stabilisation. Three transmons were read simultaneously. Multiplexing is essential for using transmons as particle detectors, since focussing on correlated errors across multiple qubits allows the disentanglement of spontaneous decay events from uncorrelated noise. The chip was directly illuminated with a pulsed LED, driven by a 15 ms-wide square signal, at a repetition rate of 1 Hz. The total energy released into the substrate by the LED was independently calibrated using the NTD-Ge thermistor glued to the chip and found to be 1.5 MeV.

A preliminary study of the multiplexed readout is fully described in [7], and will be object of future publications. The distribution of zeros is studied for the three channels acquired, in a similar fashion with respect to the previous section. The event selection is based on the simultaneous detection of a minimum number of zeros in all three channels. This threshold is determined based on the expected binomial statistics of spontaneous qubit relaxation, ensuring that selected events are unlikely to be due to random single-qubit decay. Selected events exhibit a high number of correlated errors across channels. The reconstructed event rate is $(0.902 \pm 0.004)$ events/s. Differently from the previous case, signal creation does not rely on a phonon-mediated mechanism, since Cooper-pairs in the superconducting islands are directly broken by photons emitted by the LED. In conclusion this experiment shows that illuminating a three-qubit chip with a 1.5 MeV LED, an energy comparable to particle events, induces correlated errors among the qubits in approximately 90% of cases. While this highlights the need for quantum processors to be well shielded from direct illumination, it also opens intriguing perspectives for quantum sensing.

## 6. Conclusions

This work showed that transmon qubits are subject to correlated errors induced by environmental radioactivity and cosmic rays, which lead to decoherence and quantum information loss. The same mechanism underlying these correlated relaxation events can be exploited for particle detection, where transmon qubits have the potential to operate as low-threshold detectors. Being sensitive to Cooper-pairs breaking with energy differences between levels on the order of $\mu$eV, transmons are promising candidates for rare event searches, such as light dark matter and neutrinos, offering a potential energy threshold of 0.4 eV [6].

Nonetheless, before this application of transmon qubits can be realized, it is crucial to develop robust detection protocols and selection algorithms. First, the fast detection protocol was tested on single-qubit readout. The efficiency of the selection algorithm was estimated to be $8 - 10\%$ in reconstructing events induced by radioactivity and cosmic-rays at FNAL and LNGS. Moreover, studying the dependence of the rate of selected events on the sampling period showed that the efficiency can be increased by a factor of 2 by using a faster reset protocol.

Second, the fast reset detection protocol was extended to multiplexed readout of multiple qubits. In this configuration, the chip was directly illuminated with an LED, and exploiting the simultaneous readout of three qubits, approximately 90% of LED-induced events were reconstructed as correlated signals.

Further improvements in the detection and selection algorithms, chip design, and extension of multiplexing to more qubits and chips, will provide a deeper understanding of correlated error sources, with the final goal of demonstrating the potential of transmons as next-generation particle detectors.

## References


[1] A. P. Vepsäläinen *et al.*, "Impact of ionizing radiation on superconducting qubit coherence," *Nature* **584** (2020) 551–556, doi:10.1038/s41586-020-2619-8.

[2] M. McEwen *et al.*, "Resolving catastrophic error bursts from cosmic rays in large arrays of superconducting qubits," *Nat. Phys.* **18** (2021) 107–111, doi:10.1038/s41567-021-01432-8.

[3] C. D. Wilen *et al.*, "Correlated charge noise and relaxation errors in superconducting qubits," *Nature* **594** (2021) 369–373, doi:10.1038/s41586-021-03557-5.

[4] F. De Dominicis *et al.*, "Evaluating radiation impact on transmon qubits in above and underground facilities," arXiv:2405.18355 [quant-ph] (2025).

[5] M. Bal *et al.*, "Systematic improvements in transmon qubit coherence enabled by niobium surface encapsulation," *npj Quantum Inf.* **10** (2024) 40, doi:10.1038/s41534-024-00840-x.

[6] R. Linehan *et al.*, "Estimating the energy threshold of phonon-mediated superconducting qubit detectors operated in an energy-relaxation sensing scheme," *Phys. Rev. D* **111** (2025) 063047, doi:10.1103/PhysRevD.111.063047.

[7] C. Bonomo, *First operation of superconducting quantum bits as particle detectors*, Master's thesis, Sapienza University of Rome, 2025.




PoS(14YRM2025)001